TESTING SLIP MODELS FOR TSUNAMI GENERATION

Hafize Başak Bayraktar[1,2], Antonio Scala[1] , Stefano Lorito[2], Manuela Volpe[2], Carlos Sánchez Linares[3], Gaetano Festa[1], Gareth Davies[4], Fabrizio Romano[2], Fabrizio Bernardi[2], Jacopo Selva[5], Jorge Macías[3], Marc de la Asunción[3], Manuel J. Castro[3]

(1) University of Naples Department of Physics, Napoli, Italy (hafizebasak.bayraktar@unina.it), (2) INGV, Rome, Italy, (3) Dpto. Análisis Matemático, Facultad de Ciencias, Universidad de Málaga, Málaga, Spain (4)Positioning and Community Safety Division, Geoscience Australia, Canberra, Australia, (5)INGV, Bologna, Italy

GOALS AND MOTIVATION

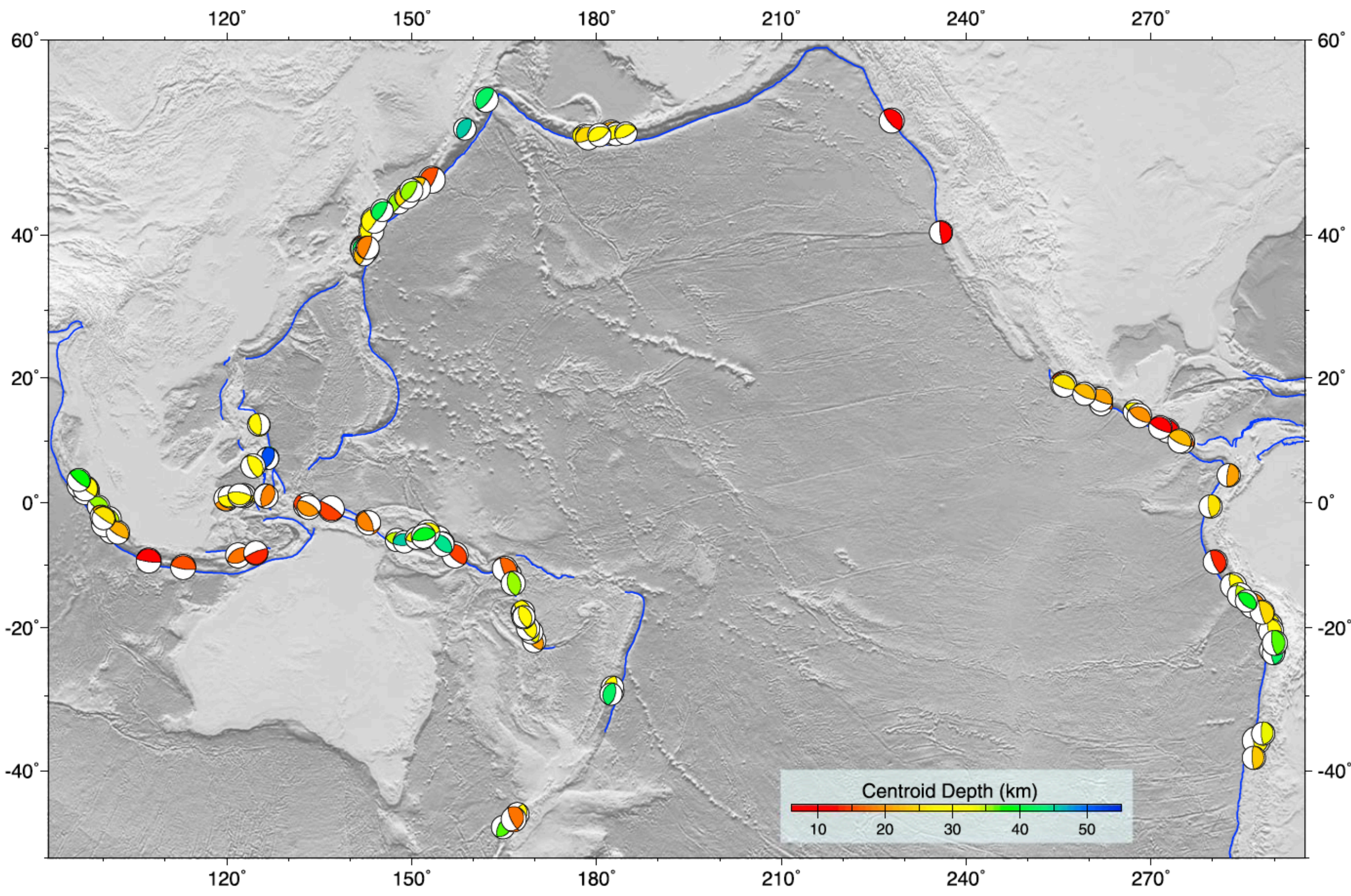

Ye et al., 2016

- Subduction zones host about 90% of historical events, including the largest ones with the magnitude M>9.
- Some of these events were followed by devastating tsunamis with, in some cases, perhaps unexpected wave height distributions.
- Hence, subduction earthquakes are a main driver for tsunami hazard, with large uncertainty associated to subduction geometry, rupture process and co-sesimic slip distribution.
- **This study focus on the uncertainty and the impact on tsunami hazard results related to stochastic heterogeneous and depth-dependent slip modelling.**

SLIP MODEL FOR TSUNAMI FORECASTING

- Numerous methods have been proposed to generate synthetic heterogenous slip distributions for tsunami hazard calculations (Davies et al., 2015; Le Veque et al., 2016; Murphy et al., 2016; Sepulveda et al., 2017; Scala et al., 2019). Slip distributions informed by kinematic models from inversion of real events are also employed (Goda et al., 2014).

- However, **it is not certain to what extent tsunami waveforms generated by these models are consistent with available tsunami observations to be used as a forecasting tool in a variety of hazard studies.**

The main goal of this study is to test synthetic tsunamis produced with different slip generation techniques, against tsunami observations from open ocean DART buoys.

STATE OF THE ART

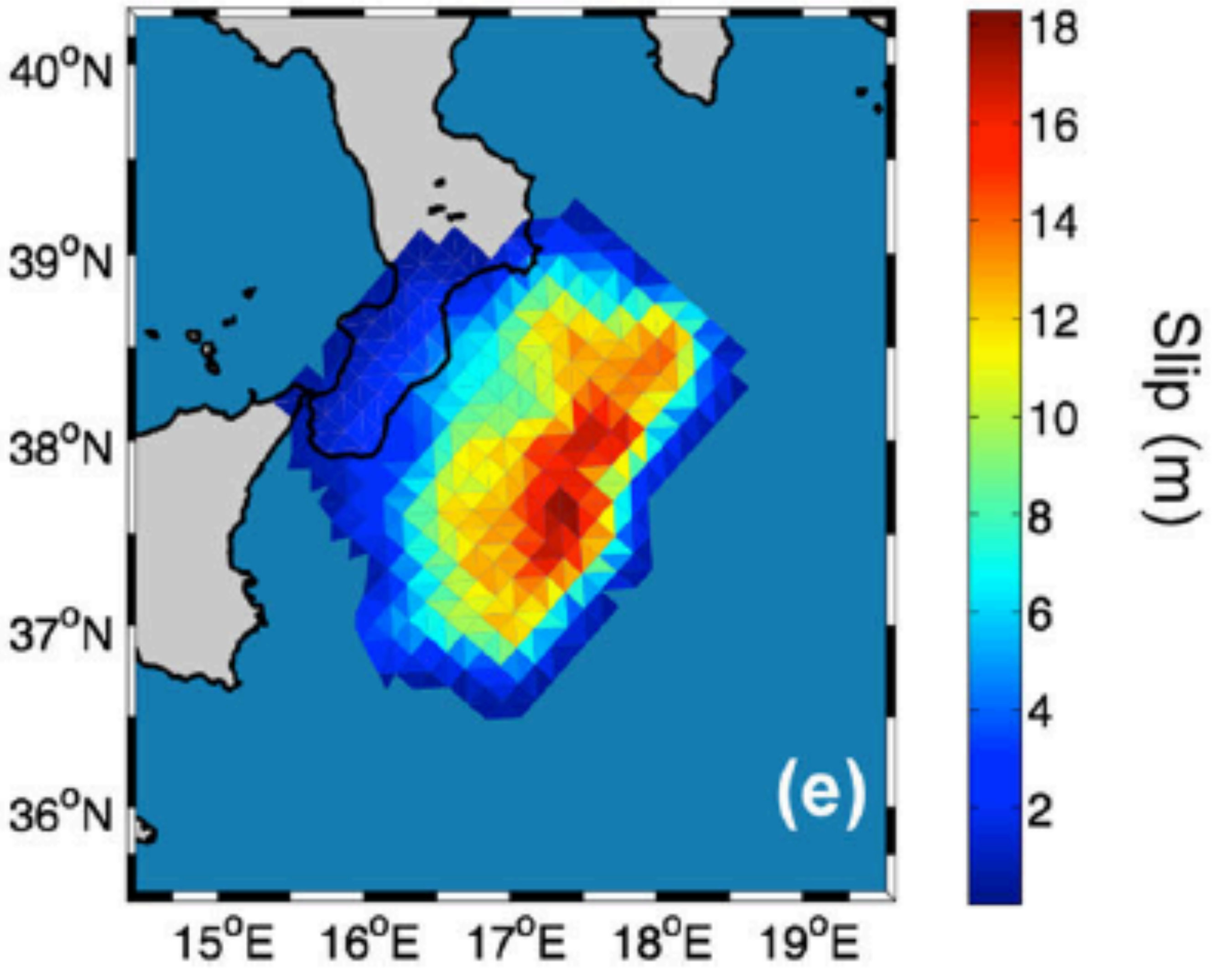

Scala et al., 2020

- A set of stochastic slip models generated by k² model.
- Earthquakes with Mw between 6.0 - 9.0.
- Shallow slip amplification is imposed depending on the variation of rigidity with depth and coupling.
- Probability of occurrence of each single event is adapted to have the total slip along the interface, in long term, equal to the relative plate convergence.

Ye et al., 2016

- The teleseismic finite-fault inversion results
- A catalog of kinematic slip models of 114 Mw≥7.0 interplate megathrust earthquakes which occurred between 1990 and 2015 on the circum-Pacific subduction zones.

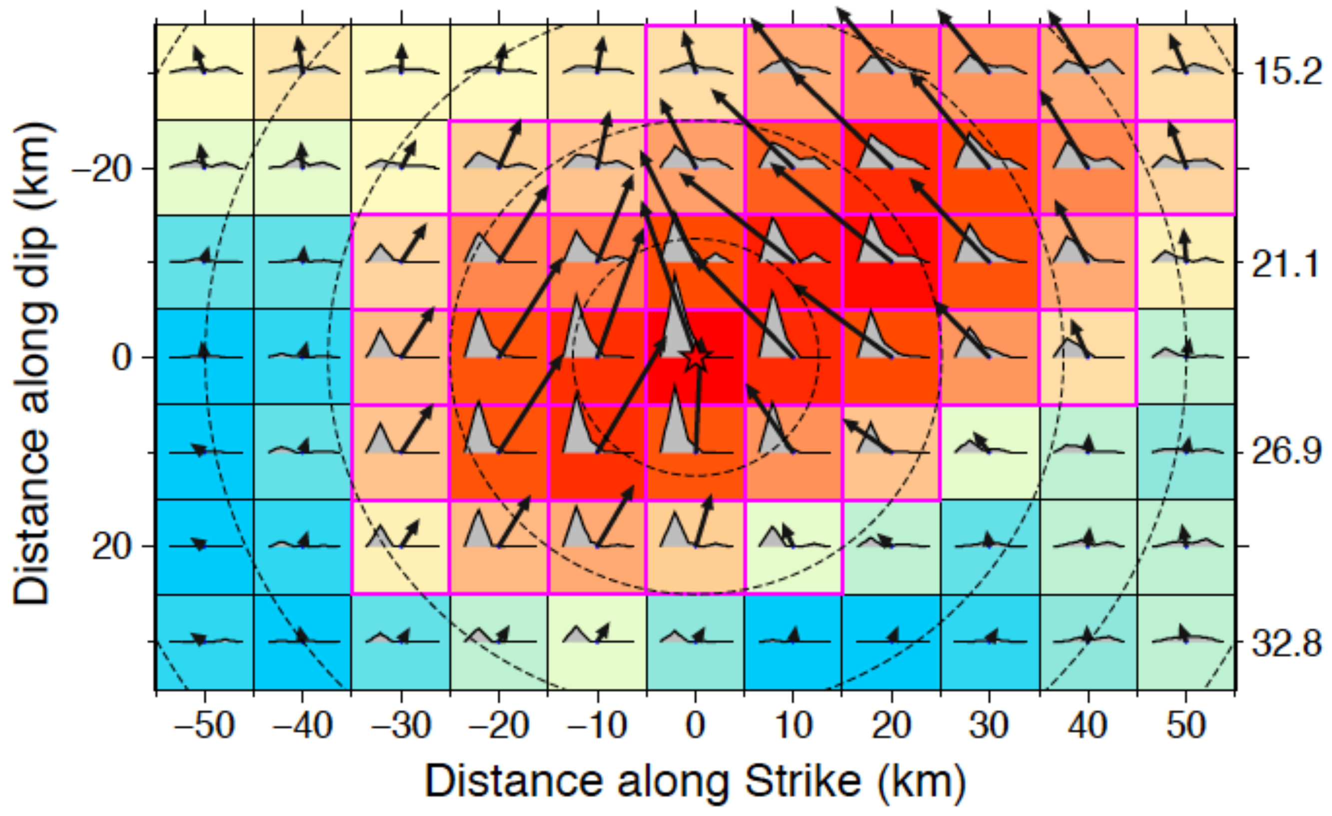

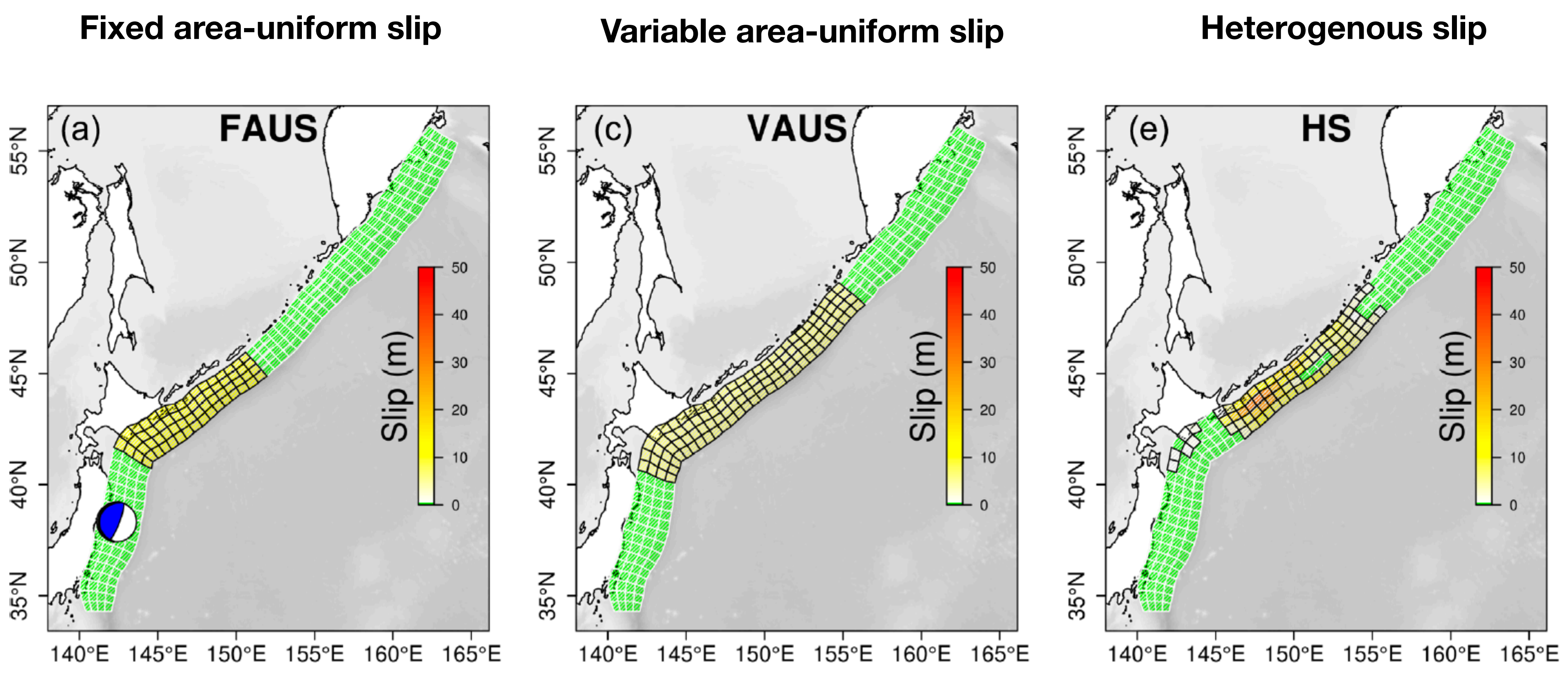

Davies, 2020

- In that study, three different models, fixed area-uniform slip, variable area-uniform slip and heterogenous slip, for tsunami source modeling in subduction zones are tested by comparing the simulated tsunami waveforms with DART records of **18 tsunami events.**
- Scenarios are generated assuming synthetic event has a similar magnitude and location of events and subduction geometry.
- Earthquake and tsunami scenarios are generated for both depth-independent (constant rigidity) and depth-dependent (rigidity varies with depth) cases.

TESTING TSUNAMI SOURCE MODELS

Davies (2019) proposes some criterions for comparison of tsunamis generated by models and Darts observations.

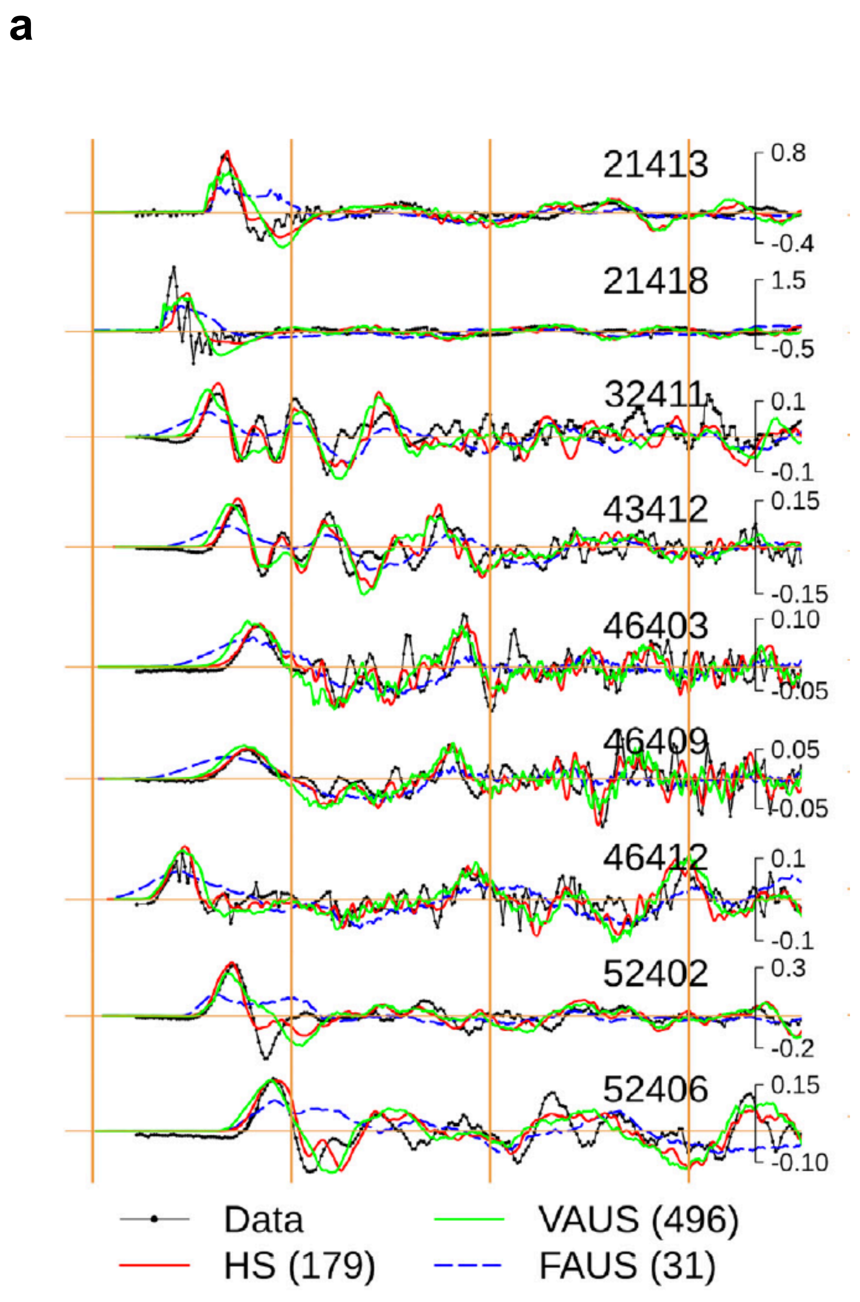

Davies, 2019

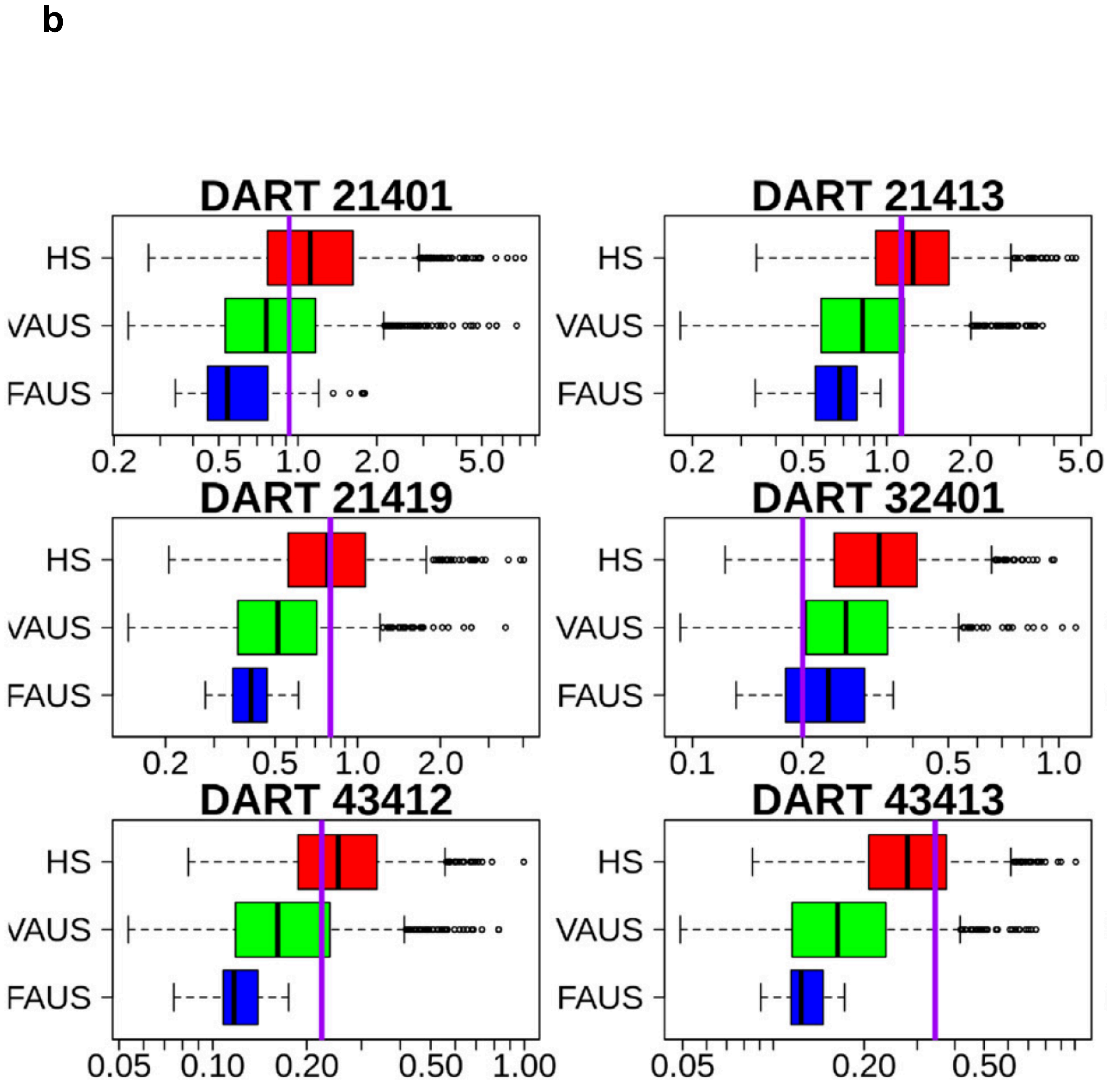

- First of all, a goodness-of-fit criterion is developed to identify stochastic scenarios which generates most similar behavior to the observed tsunamis (Figure a).
- The statistical properties of the tsunami stage-range (difference between the max. and min. tsunami wave height) for scenarios are compared to analyze biases in the representation of tsunami size by the different models with the de-tided stage-range observed during the event (Figure b).
- The techniques provided by this study to compare model results with real observations can be applied to test other stochastic tsunami scenario generation techniques to identify and partially correct biases of these scenarios, and provide better justification for their use in applications.

AIM OF THE STUDY

In this study, to further progress along similar lines, we compare synthetic tsunamis produced by kinematic slip models obtained by recent stochastic slip generation techniques (Scala et al., 2020) against tsunami observations at open ocean DART buoys, for the 15 earthquakes, during the period 2006–2016 in the Global Centroid Moment Tensor (GCMT) catalogue with hypocentral depths≤71 km and moment magnitudes Mw>7.7, and ensuing tsunamis analyzed by Davies (2019). Given the magnitude and location of the real earthquakes, we consider ensembles of consistent slipping areas and slip distributions, accounting for both constant and depth-dependent rigidity models.

Kinematic slip models on planar faults obtained with tele-seismic inversion for 13 out of 18 events, considered by Davies (2019), are also present in the earthquake catalog of Ye et al. (2016).

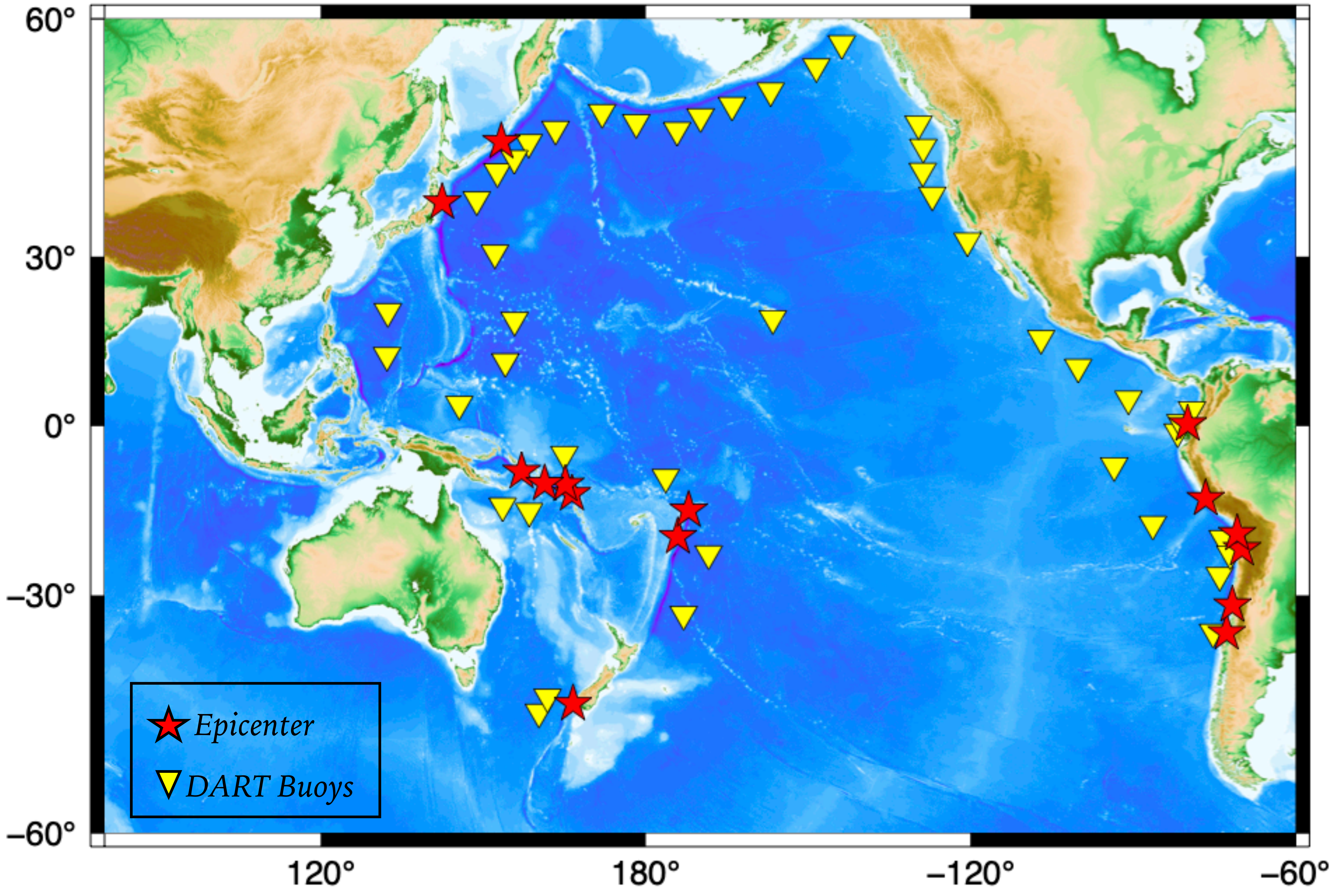

Location of the events and Dart buoys

AIM OF THE STUDY–EVENT LIST

Event Name	Event-ID	Date	Number of DART	Mw	Lon	Lat	Depth (km)
Kermadec-Tonga	KT1	2006/05/03 15:26:40.3	1	8.0	-174.12	-20.19	55.0
Kurils-Japan	KJ1	2006/11/15 11:14:17.8	12	8.3	153.29	46.57	38.9
Solomon	So1	2007/04/01 20:39:56.4	2	8.1	157.04	-8.46	10.0
Peru	SA1	2007/08/15 23:40:57.9	3	8	-76.60	-13.39	39.0
Chile	SA2	2007/11/14 15:40:50.5	2	7.8	-69.89	-22.25	40.0
New Zealand	Pu1	2009/07/15 09:22:29.0	2	7.8	166.56	-45.76	12.0
Kermadec-Tonga	KT2	2009/09/29 17:48:11.0	5	8.1	-172.10	-15.49	18.0
Vanuatu	NH1	2009/10/07 22:18:51.2	1	7.8	166.38	-12.52	35.0
Chile	SA3	2010/02/27 06:34:15.6	16	8.8	-72.71	-35.85	44.8
Tohoku	KJ2	2011/03/11 05:46:23.0	28	9.1	142.37	38.32	24.4
Santa Cruz	NH2	2013/02/06 01:12:25.8	5	7.9	165.11	-10.80	24.0
Northern Chile	SA4	2014/04/01 23:46:47.3	7	8.2	-70.77	-19.61	25.0
South-America	SA5	2015/09/16 22:54:32.9	18	8.3	-71.67	-31.57	22.4
South-America	SA6	2016/04/16 23:58:36.9	2	7.8	-79.93	0.35	21.0
Solomons	So2	2016/12/08 17:38:46.3	3	7.8	161.32	-10.68	40.0

List of the events used in slip model generation

TSUNAMI-HYSEA

- *Tsunami-HySEA* model is used to perform tsunami numerical simulations. The model implements in the same code the three parts of an earthquake generated tsunami: generation, propagation, and coastal inundation. In the generation stage, Okada's fault deformation model (Okada, 1985) is used to predict the initial bottom deformation that is transmitted instantaneously to the sea surface generating the tsunami wave.
- *Tsunami-HySEA* uses the **2D nonlinear one-layer shallow water system** in both spherical and Cartesian coordinates.
- It has passed all laboratory tests and proposed benchmark problems (Millán, A. (2014), Macías et al. (2016a, b)).

FASC TOOL- ON-THE-FLY SLIPPING AREAS AND EARTHQUAKE SCENARIOS

Preprocessing

Subduction slab triangular elements

24 slabs in the Pacific

```
{"zone_name": "kurilsjapan",
        "Merc_zone": 54,
        "acronym": "KuJ",
```

```
"Configure": {
"application": "PTF",
"shape": "Circle",
"preprocess": 1,
"Magnitude_lb": 0.15,
"Magnitude_ub": 0.15,
"minimum_bnd_distance": 0.5,
"minimum_interdistance": 0.1,
"hypo_baryc_distance": 1,
"Fact_area_scaling": 1
```

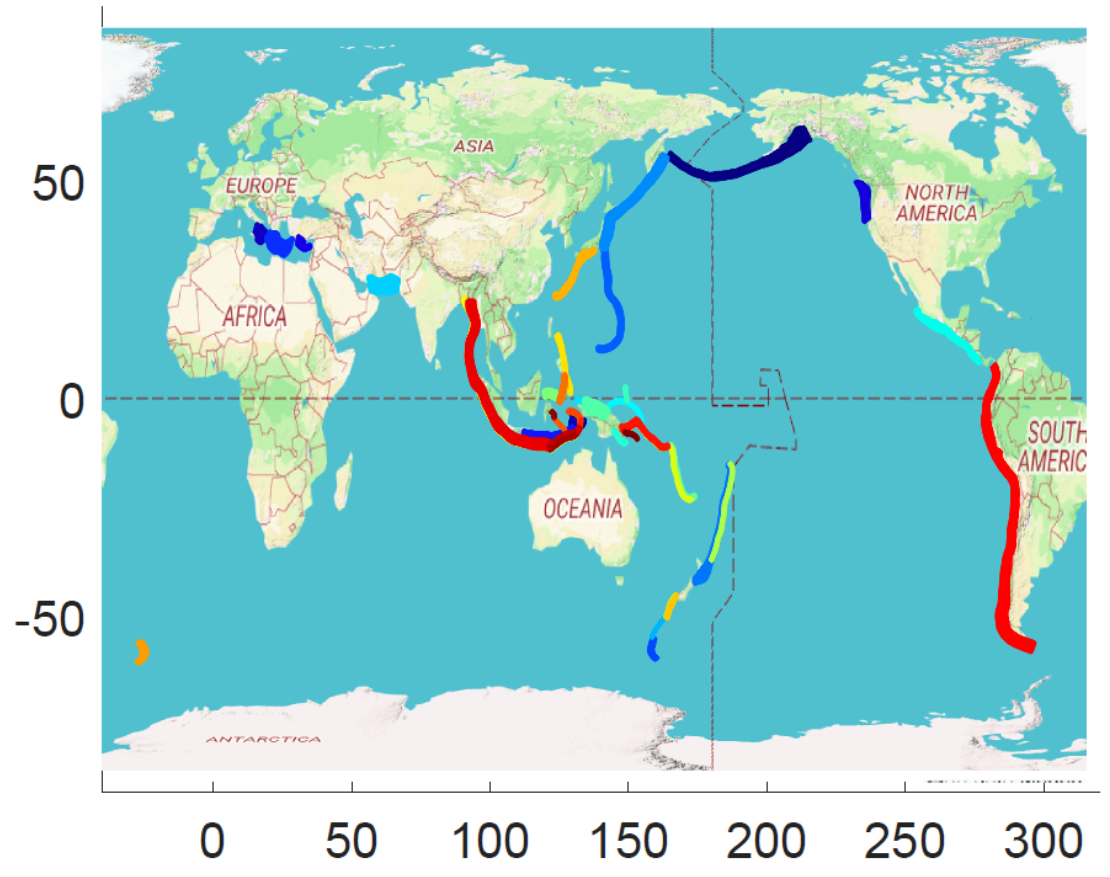


```
"Event": {
"Name": "Kurils-2006",
"Hypo_LonLat" : [153.29, 46.57],
"Magnitude" : 8.3
```

A possible active set of barycentres, geometrical centers of the modeled subduction earthquakes to be included in the ensemble.

These barycenters are selected using the similar earthquake location and magnitude assumption proposed by Davies., 2020.

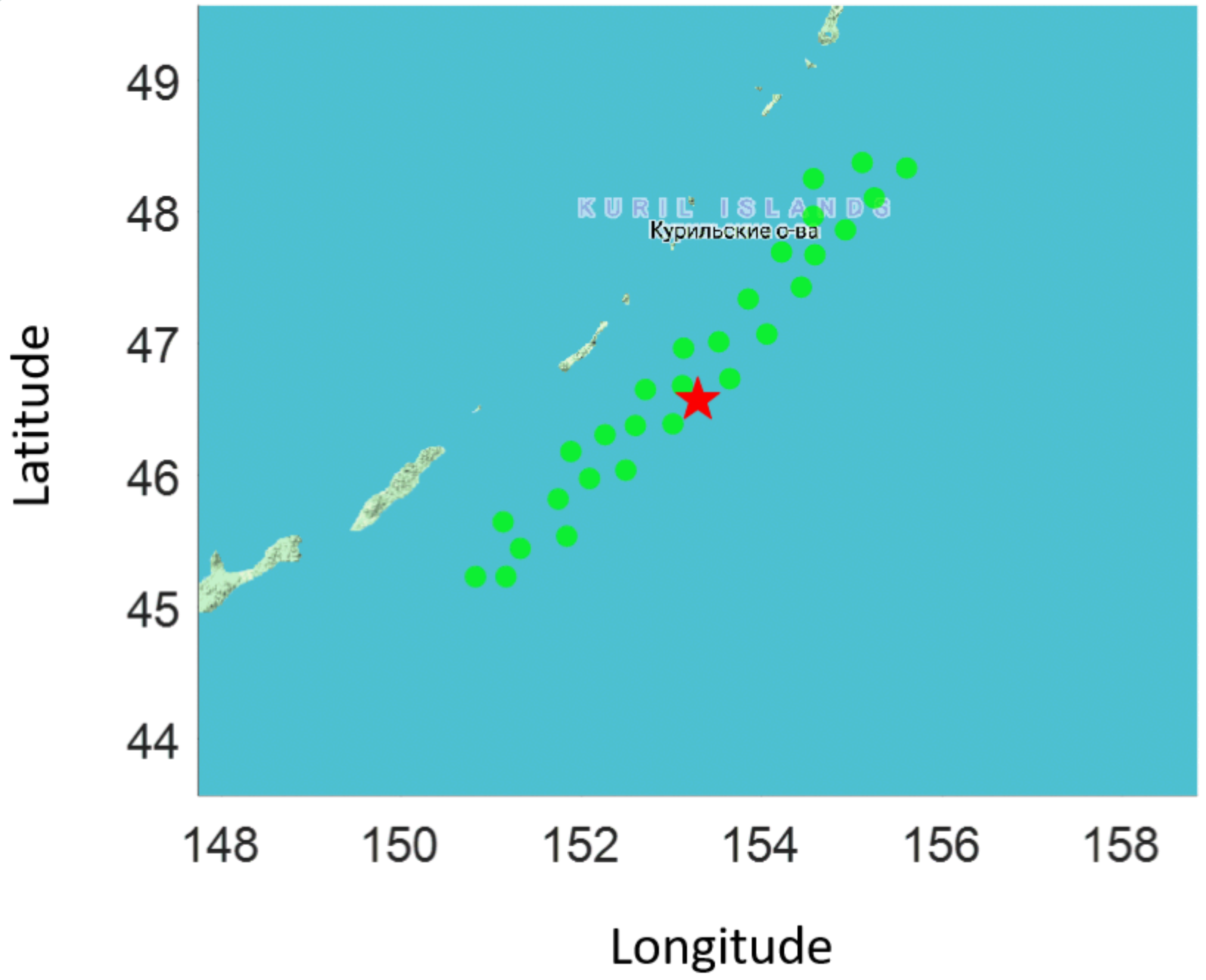

FASC TOOL- ON-THE-FLY SLIPPING AREAS AND EARTHQUAKE SCENARIOS

Preprocessing

Subduction slab triangular elements

24 slabs in the Pacific

```
{"zone_name": "kurilsjapan",
        "Merc_zone": 54,
        "acronym": "KuJ",
```

```
"Configure": {
"application": "PTF",
"shape": "Circle",
"preprocess": 1,
"Magnitude_lb": 0.15,
"Magnitude_ub": 0.15,
"minimum_bnd_distance": 0.5,
"minimum_interdistance": 0.1,
"hypo_baryc_distance": 1,
"Fact_area_scaling": 1
```

+

```
"Event": {
"Name": "Kurils-2006",
"Hypo_LonLat" : [153.29, 46.57],
"Magnitude" : 8.3
```

Circular

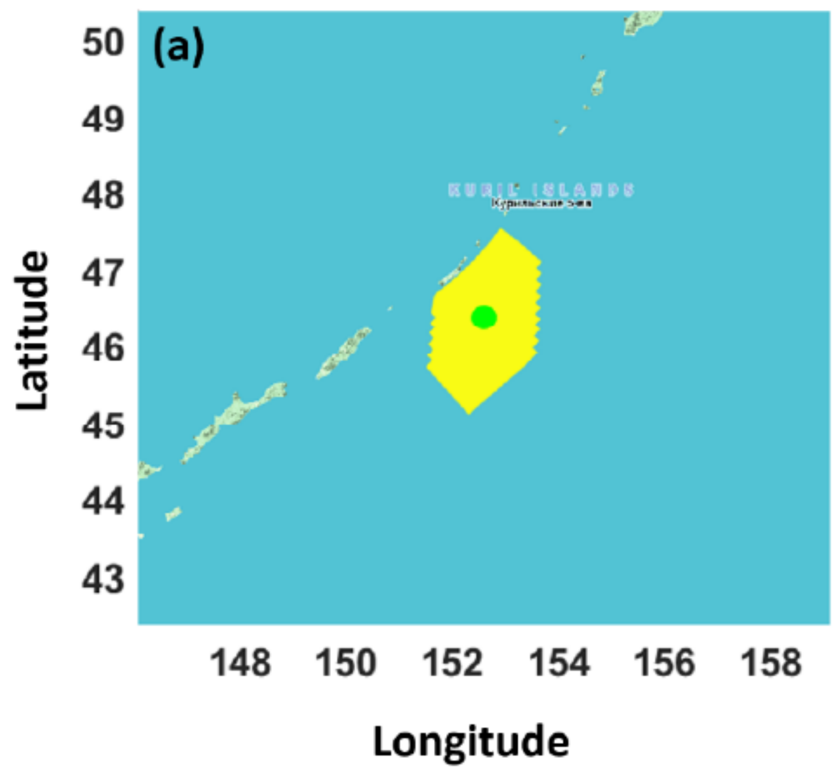

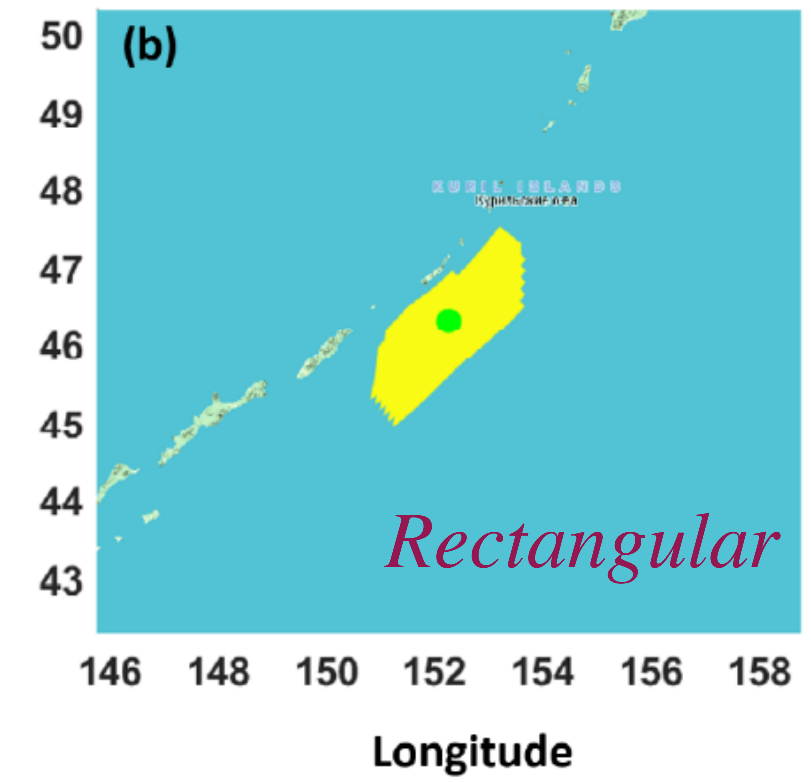

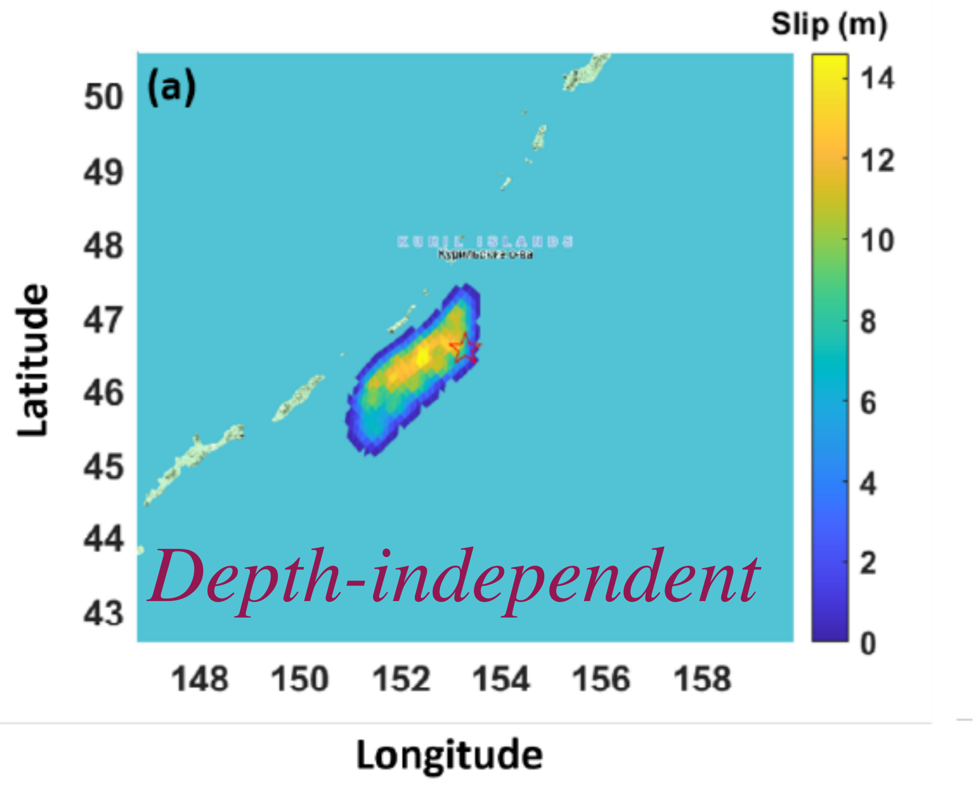

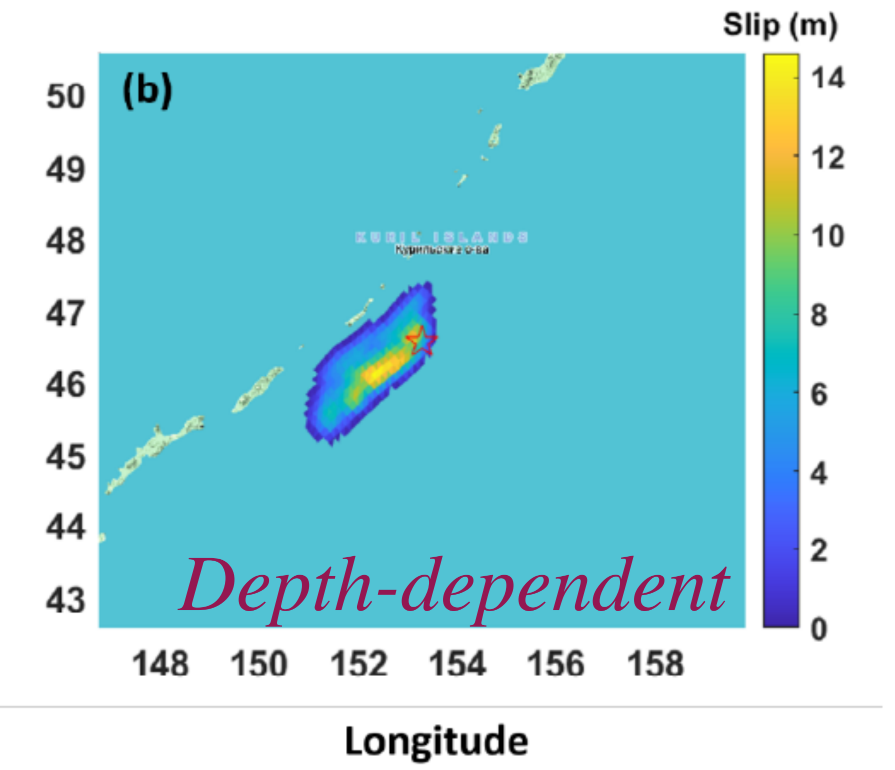

4 different rupture areas for each of the selected barycentres are defined,

- 2 different empirical scaling relations (Murotani et al. 2010; Strasser et al. 2011).
- 2 different rupture shapes, one approximately circular and one with an aspect/ratio controlled by L/W as prescribed by the scaling relations.

Using the approach proposed by Scala et al. (2020)

FASC TOOL- ON-THE-FLY SLIPPING AREAS AND EARTHQUAKE SCENARIOS

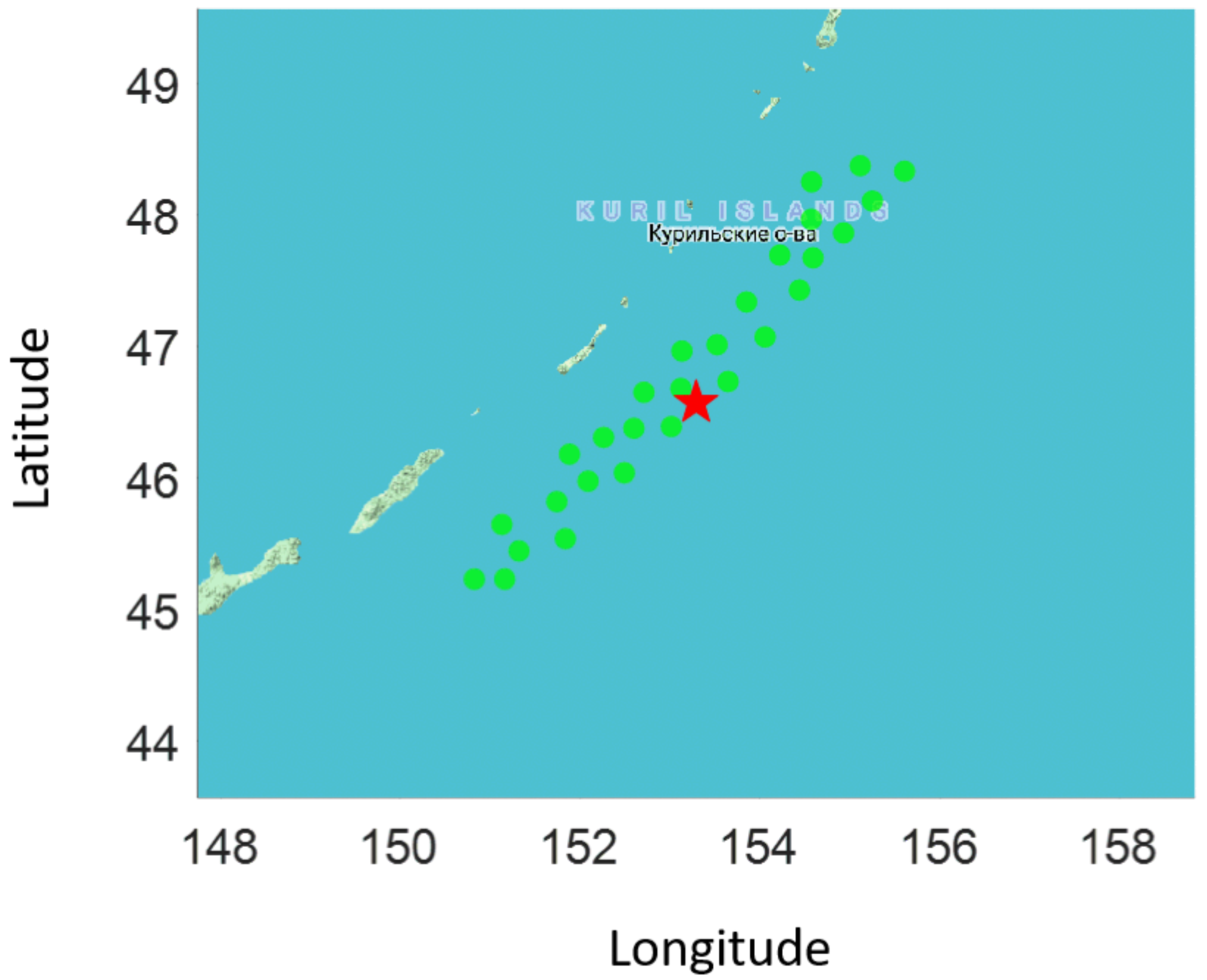

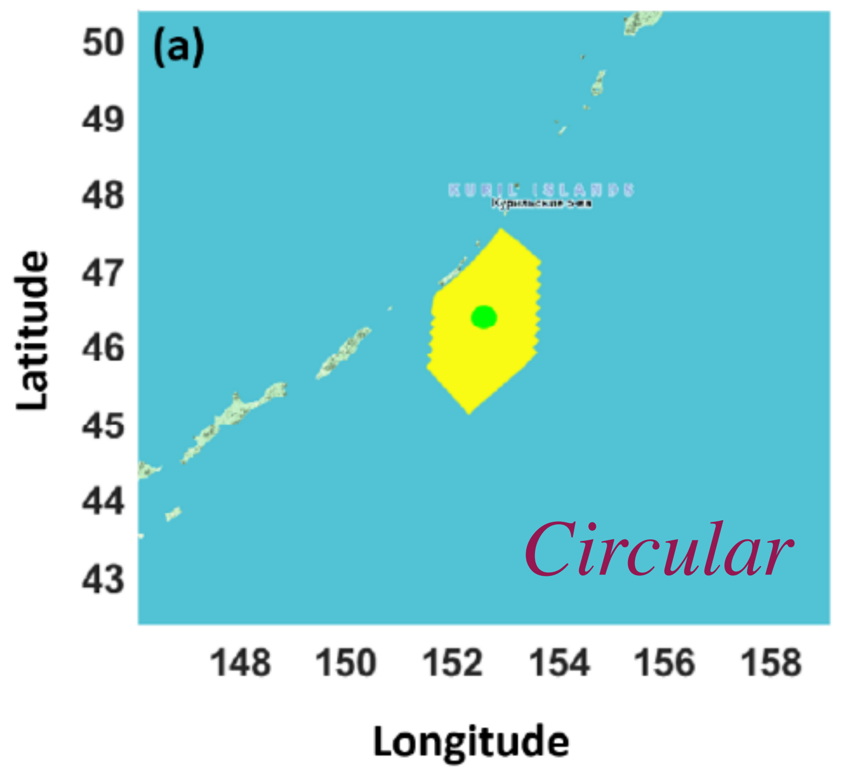

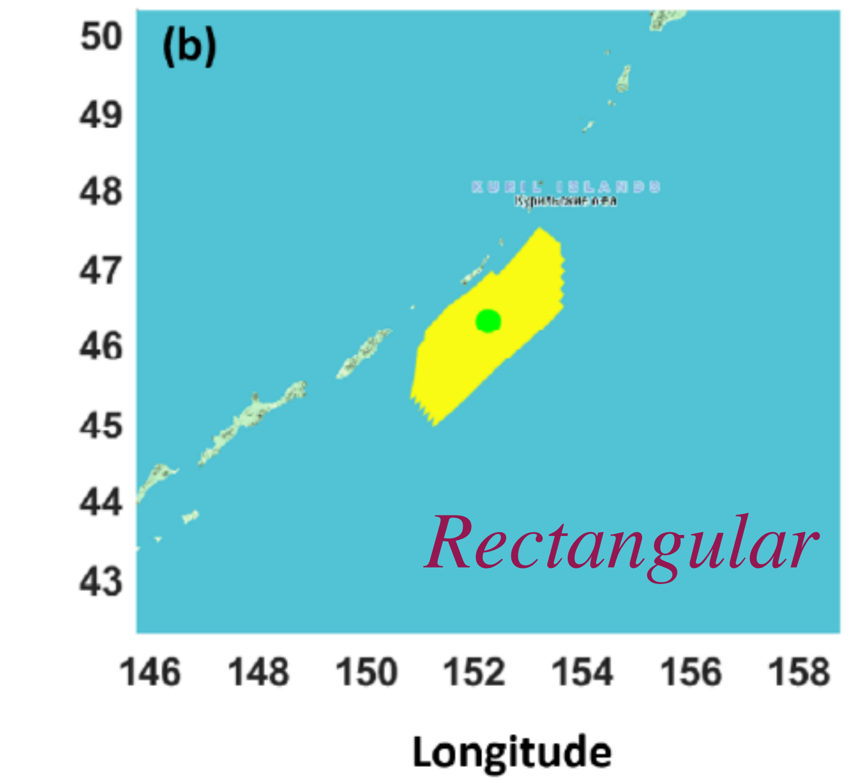

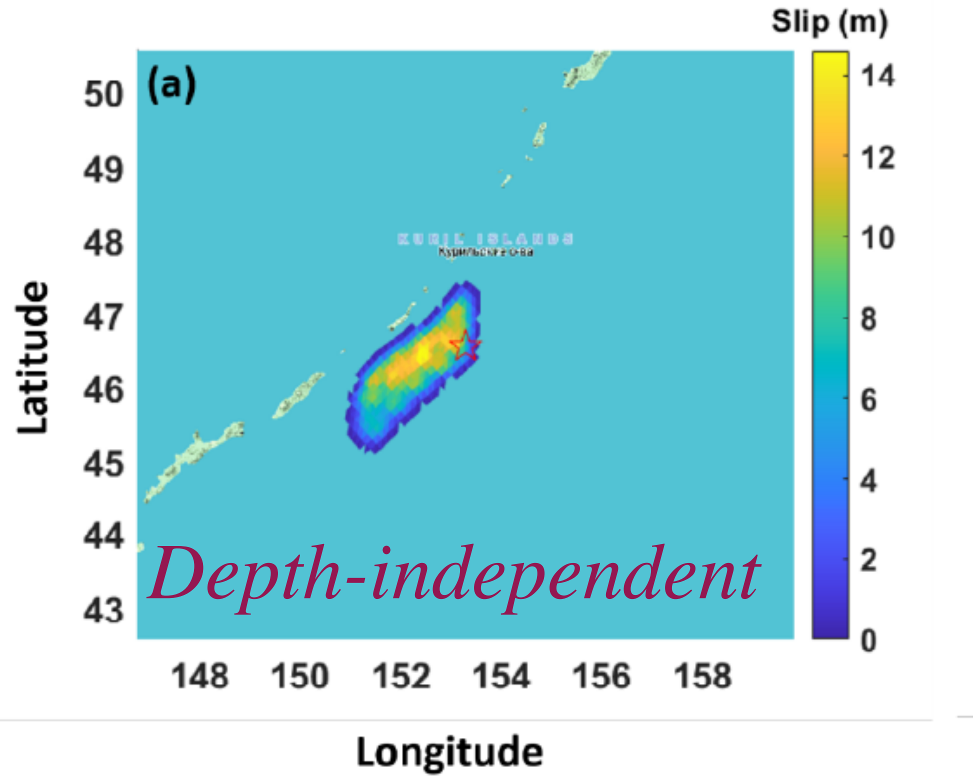

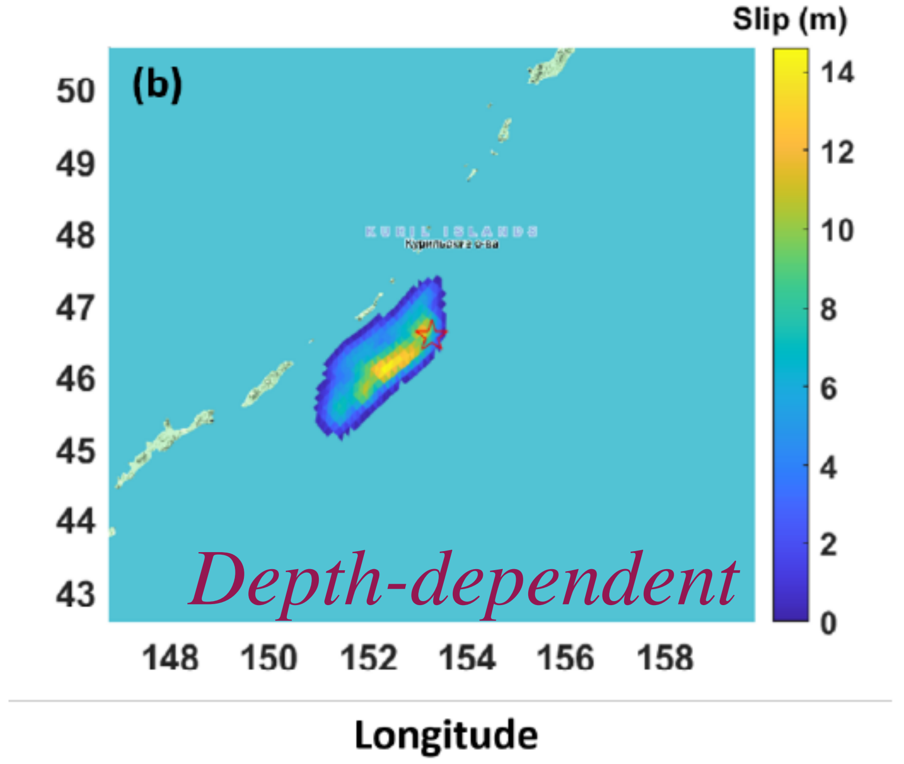

TESTING TSUNAMI SOURCE MODELS-GOODNESS OF FIT STATISTICS

For each scenario 'scenario goodness-of-fit statistic' (G_e^s) shows the agreement with DART buoy observations from the observed event. This statistic can be defined as a cost function where *obs(t$_i$)* and *syn(t$_i$)* defines the time-series for observation and synthetic model, respectively. t_i is a time sequence limited to between the beginning and end of high-frequency DART sampling. Definition of the scenario goodness-of-fit statistic starts with consideration of a single Dart station and then for each model, goodness-of-fit ($G_{e,d}^s$) should be calculated. Goodness-of-fit varies between 0-2 with lower values indicating a better fit.

$$G_{e,d}^s = 1 - \left(\frac{2 * (\sum_i obs(t_i) * syn(t_i))}{\sum_i obs(t_i)^2 + \sum_i syn(t_i)^2}\right)$$

$$G_e^s = median(G_{e,d}^s)$$

$e = Observed\ event$

$d = Dart\ buoy$

$s = Scenario$

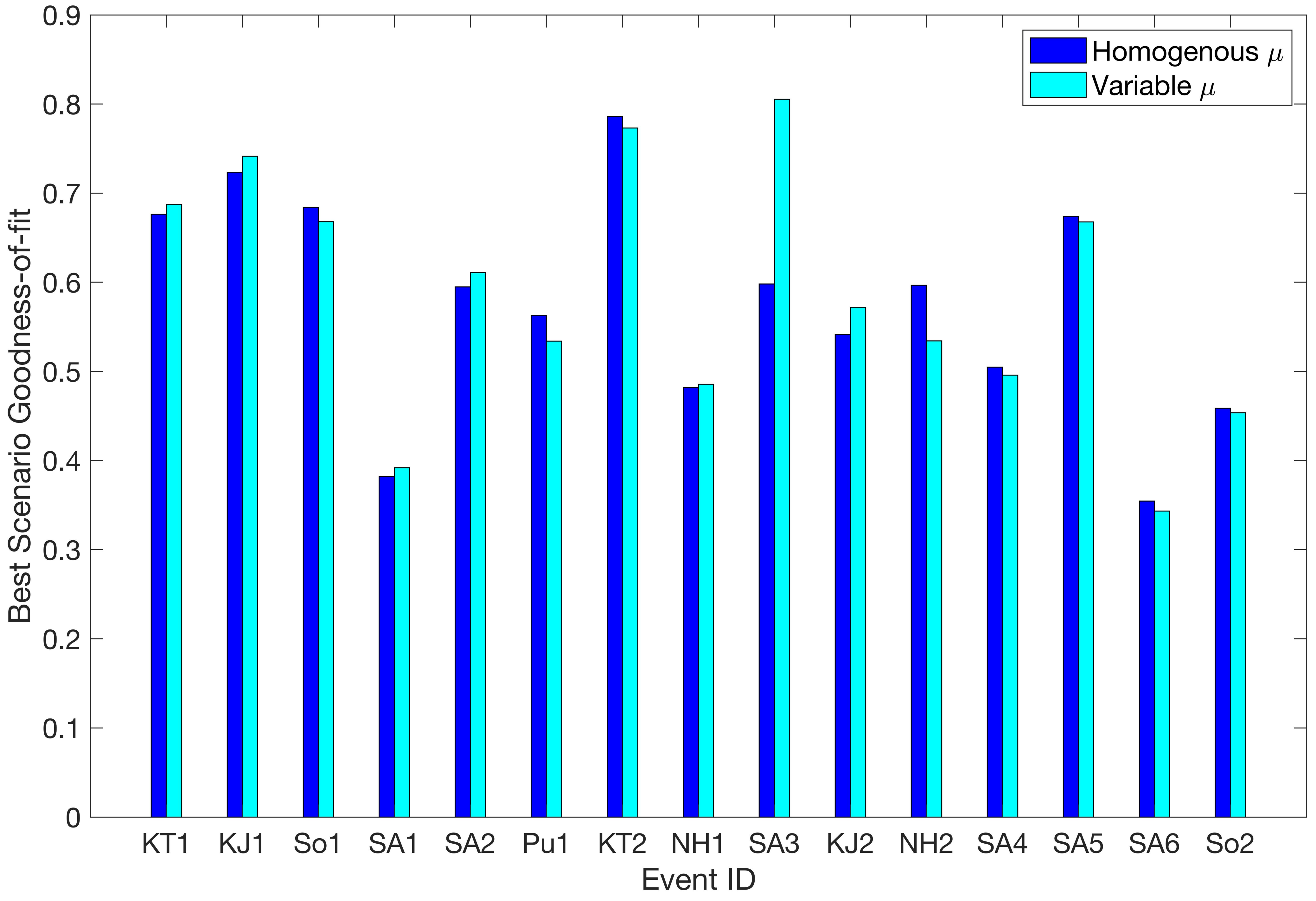

TESTING TSUNAMI SOURCE MODELS–COVERAGE STATISTICS

Coverage statistic ($F^{m}_{e,d}$) is the fraction of model scenarios that have smaller stage-range than the observation at the Dart buoy. This statistics defines how big the observed tsunami relative to the model scenario.

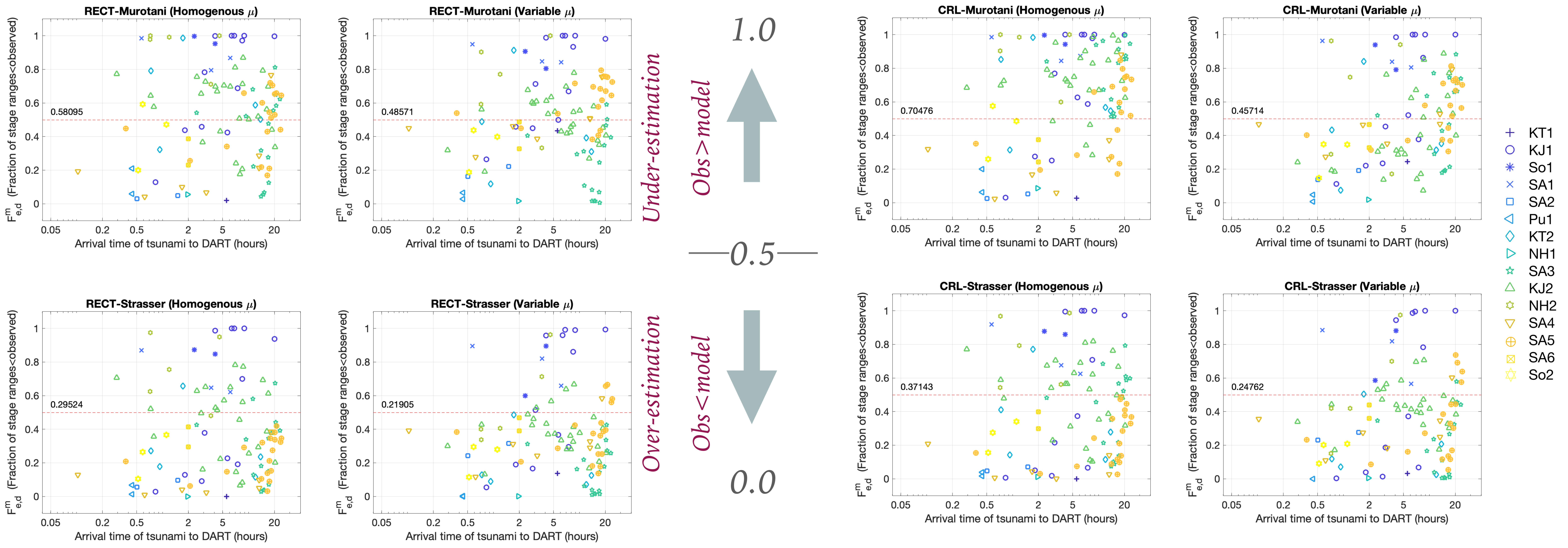

PRELIMINARY RESULTS

- ✦ The best scenario goodness of fit statistics indicates rigidity independent behaviour for each event, except 2010-Maule event, which shows better agreement between the model scenarios and observations for depth-independent rigidity case.

- ✦ Coverage statistic results show that models generated using Murotani et al. (2013) scaling law and rectangular shaped rupture show model scenarios and observations have relatively similar stage-ranges while the models generated by Strasser et al. (2010) scaling law over estimates the observations.

WHAT IS NEXT?

- ✦ Best scenario goodness of fit will be calculated for all 8 different model classes, to address better what are the source features that lead to a better fit with observations.

- ✦ Comparison of tsunami generated by the teleseismic inversion results of Ye et al. (2016) with tsunami records and other model results should be done.

- ✦ Model calibration will be done by the techniques proposed by Davies and Griffin (2020) when comparison of models are done.